Assessing and optimizing the role of wind forcing and upper-ocean dynamics in marine pollution transport simulations using surface drifters in the Canary Current System

Álvaro Cubas[1], Francisco Machín[2*], Daura Vega-Moreno[3], Eugenio Fraile-Nuez[4*] and Borja Aguiar-González[5]

[1]University of Las Palmas de Gran Canaria, Las Palmas de Gran Canaria, 35017, Spain
[2]Oceanografía Física y Geofísica Aplicada (OFYGA), IU-ECOAQUA, University of Las Palmas de Gran Canaria, 35017, Spain
[3]OpenPLAS Group, Chemistry Department, University of Las Palmas de Gran Canaria, Las Palmas de Gran Canaria, 35017, Spain
[4]Centro Oceanográfico de Canarias, Instituto Español de Oceanografía (IEO), Consejo Superior de Investigaciones Científicas (CSIC), Santa Cruz de Tenerife, 38180, Spain
[5]EOMAR, IU-ECOAQUA, University of Las Palmas de Gran Canaria, Las Palmas de Gran Canaria, 35017, Spain

Correspondence to: Francisco Machín (francisco.machin@ulpgc.es) and Eugenio Fraile-Nuez (eugenio.fraile@ieo.csic.es)

Abstract.

This study investigates the sensitivity of undrogued drifter trajectory simulations in the Macaronesia region, selected for their similarity to the behavior of marine litter transport in the upper ocean. The research evaluates the influence of various physical processes, including advection schemes, horizontal dispersion, windage and Stokes drift. A total of 320 simulations were conducted, incorporating different combinations of these processes, the modeled trajectories were compared with real drifter data. The analysis demonstrated that the inclusion of windage and/or Stokes drift significantly improved the agreement between modeled and observed trajectories, particularly when windage factors (WDF) ranged from 2.5% to 5%. Horizontal dispersion exhibited minimal influence on the trajectories, indicating that turbulent diffusion had a limited effect under the study conditions. While both advection schemes (RK2 and RK4) produced comparable results, RK4 outperformed RK2 in scenarios involving pronounced mesoscale activity. This research highlights the relevance of using undrogued drifters to mimic marine litter transport and underscores the importance of incorporating windage and/or Stokes drift in trajectory simulations, particularly in regions like Macaronesia, where mesoscale processes play a critical role.

1 Introduction

Marine pollution by microplastics is arguably one of the most pressing environmental challenges of our time. Addressing this issue requires a multidisciplinary approach that integrates a physical, chemical, and biological perspectives along with

economic, social, and political dimensions (McGlade et al., 2021). The perspective of physical oceanography plays a key

35   role in uncovering the pathways of marine pollutants, identifying their accumulation zones, and determining their residence times. This information is critical not only for understanding the impact on marine ecosystems but also for providing essential tools to manage environmental crises in real time.

Once the marine litter enters the environment, reliable tools for effectively tracking its movement remain lacking. Instead, its behavior can be simulated by deploying virtual particles that mimic the dynamics of actual marine litter under specific

40   environmental conditions (Castro-Rosero et al., 2023; Declerck et al., 2019; Jalón-Rojas et al., 2019). Such Lagrangian simulations typically require the inclusion of several parameters and complex equations that account for the major physical processes governing ocean dynamics. A common approach to evaluate the significance of these parameters or processes is sensitivity analysis, which provides insights into how variations in inputs $x=(x_1,x_2,...,x_n)$ affect the output y. Inputs may include ocean currents, wind stress, number of particles, grid resolution, dispersion and drag coefficients, among others,

45   while y might represent the position of the particles at a specific location and time or the length of the impacted shoreline. Both inputs and outputs depend on the specific study being conducted and the framework used to calculate the trajectories, such as TrackMPD (Jalón-Rojas et al., 2019), OceanParcels (Lange and Sebille, 2017), PaTATO (Fredj et al., 2016) or OpenDrift (Dagestad et al., 2018), among others.

Here, we present a sensitivity analysis in the Canary Current System, comparing simulated trajectories with observed

50   surface drifter trajectories to identify the optimal parameter values that best capture the physical processes governing the marine pollution transport in the region.

The circulation pattern in this system is predominantly influenced by the general circulation of the North Atlantic subtropical gyre, particularly its eastern branch, the Canary Current. This equatorward flow interacts with coastal upwelling waters and geographical structures such as the Canary Islands archipelago. The Canary Current exhibits strong seasonality,

55   intensifying during spring and summer before shifting offshore in fall (Machín et al., 2006; Mason et al., 2011; Pérez-Hernández et al., 2013; Stramma and Siedler, 1988).

Additionally, an equatorward coastal upwelling jet, known as the Canary Upwelling Current, originates north of Cape Ghir (Pelegrí et al., 2006). This current intensifies during spring (Machín and Pelegrí, 2006) and flows along the coast during spring and summer, driven by the seasonal variability of the prevailing winds (Cropper et al., 2014; Pelegrí et al., 2005)

60   The presence of the Canary Archipelago, which interrupts the main flow of the Canary Current generates significant mesoscale activity. This includes vortex streets downstream of the islands, creating a consistent pathway for eddies, known as the Canary Eddy Corridor (Sangrà et al., 2009). Numerous upwelling filaments are also present, some of which are quasi-permanent features (Arístegui et al., 1997; Barton et al., 1998).

Reversals in the main flow have been observed near the Canary-Coastal Transition Zone during late autumn and winter

65   (Navarro-Pérez and Barton, 2001). These flow changes are likely caused by a weakening of the trade winds south of Cape Ghir (Pelegrí et al., 2005), which allows the development of a northward flow between Cape Blanc and Cape Juby (Hernández-Guerra et al., 2002; Machín and Pelegrí, 2009). In addition, the interaction of the trade winds with the islands

diverts airflow to the flanks, creating warm wakes and altering surface circulation in the lee regions (Barton et al., 2000; Basterretxea et al., 2002; Hernández Guerra, 1990).

Regarding wind patterns, the region between 20º and 30ºN experiences year-round upwelling-favorable wind stress along the northwest African coast (Bakun and Nelson, 1991). Furthermore, the Canary Islands region (28º-29ºN) is periodically affected by intermittent pulses of dust clouds from North Africa, known as *calima*, which peak mainly in winter and summer/autumn (Torres-Padrón et al., 2002).

The objectives of this research are to investigate the influence of multiple oceanographic and meteorological processes, such as wind forcing and Stokes drift, on the trajectories of surface drifters in the Canary Current System. This is achieved by comparing observed trajectories with those modeled trajectories using TrackMPD. By conducting a sensitivity analysis, we aim to identify the optimal parameter values for the most accurate trajectory modeling. This approach not only clarifies the role of each process but also addresses challenges in parameter estimation, ultimately enhancing the replication of pollutant transport dynamics in the region.

2 Material and Methods

2.1 Drifters data

We utilized satellite-tracked drifters from the hourly drifter data provided by the Global Drifter Program (GDP) (Elipot et al., 2016, 2022). These buoys, with a half-life of 1.5 to 2 years, employ Iridium SBD telemetry and are equipped with a 6-meter Holey sock drogue centered at 15 meters depth. The drifters are constructed using two hemispheres of acrylonitrile butadiene styrene (ABS), forming a spherical float. Additionally, they are fitted with strain gauges to detect whether the drogue remains attached. Detailed specifications for each selected drifter are provided in Table 1.

Table 1. Specifications of selected drifters. ID: GDP identification number; WMO: World Meteorological Organization identifier; SVPB: Surface Velocity Program Barometer; SVP: Surface Velocity Program.

Name	ID	WMO	Experiment Number	Buoy Type	Diameter (cm)	Manufacturer	Manufacture Year
TR1	300234065704790	4101609	21321	SVPB	35.5	PacificGyre	2016
TR2	300234065749810	4101717	21321	SVPB	40	MetOcean	2016
TR3	300234066214360	6203843	21421	SVPB	35.5	Pacific Gyre	2020
TR4	300234066797700	4401580	2222	SVPB	40	MetOcean	2019
TR5	300234066892260	6203634	2222	SVPB	40	MetOcean	2019
TR6	300234067973120	6203776	21321	SVPB	35.5	Pacific Gyre	2020

Name	ID	WMO	Experiment Number	Buoy Type	Diameter (cm)	Manufacturer	Manufacture Year
TR7	300234068245900	6203597	21312	SVP	38.1	SIO	2019
TR8	300534060651930	4402660	21312	SVPB	39	DBi	2020
TR9	300534061170370	6204561	2222	SVPB	40	NKE	2020
TR10	300534061655130	1301717	21421	SVPB	35.5	Pacific Gyre	2020

90   We selected drifters with trajectories passing near the Canary Islands and Madeira archipelagos, within a latitude range of 27ºN to 34ºN and a longitude range of 19ºW to 8ºW, over the temporal domain off 2021 to 2022. The data were further filtered to include only trajectories where the drogue had already been lost, ensuring proper consideration of windage effects (Brügge and Dengg, 1991; Pazan, 1996). From this dataset, we identified 10 trajectories (TR_i), to capture a variety of physical processes that could either hinder or facilitate the trajectory computation (Figure 1). To assist in the selection, we

95   computed key trajectory characteristics such as duration, effective distance, track stability (the ratio of effective distance to total distance), and others (Table 2).
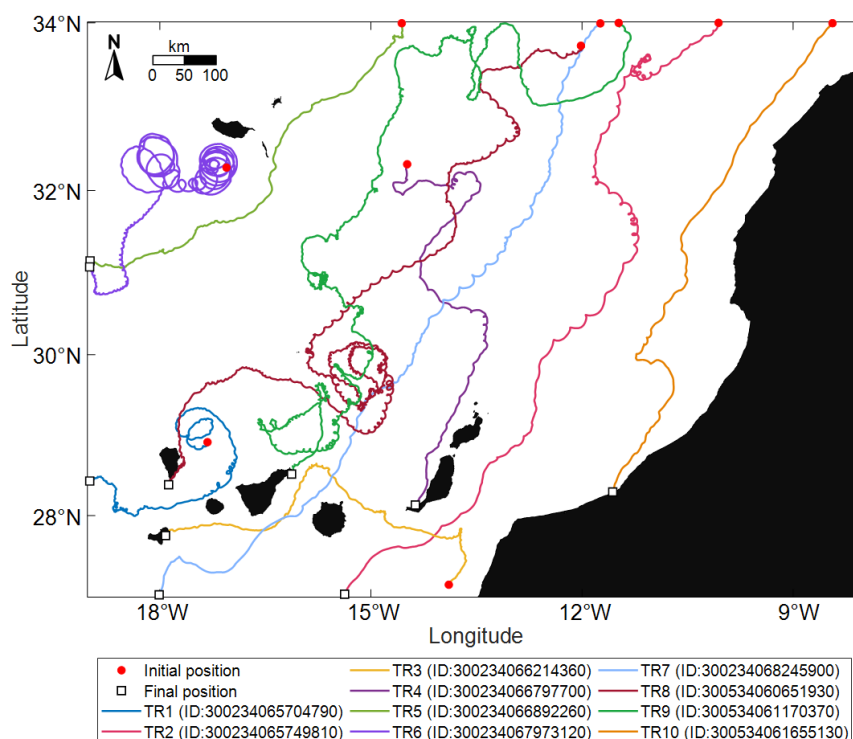

Figure 1. Trajectories of the selected undrogued drifters (TR) used in the sensitivity analysis.

100   **Table 2. Characteristics of the selected drifters' trajectories (TR)**

Name	Drogue Lost Date	In Domain First Date	In Domain Last Date	Trajectory duration (Days)	Distance (km)	Effective Distance (km)	Track Stability	Mean Velocity (m/s)
TR1	30/01/2020	03/04/2021	30/05/2021	57.21	781.99	171.88	0.22	0.16
TR2	02/10/2019	04/05/2022	24/06/2022	51.38	1421.31	928.98	0.65	0.32
TR3	25/12/2021	25/12/2021	06/02/2022	43.13	674.96	403.21	0.60	0.19
TR4	14/04/2020	03/04/2021	11/05/2021	38.63	832.38	465.47	0.56	0.25
TR5	10/06/2021	24/09/2021	26/10/2021	31.92	638.42	521.91	0.82	0.23
TR6	05/07/2021	05/07/2021	02/10/2021	89.17	2423.17	227.42	0.09	0.26
TR7	09/07/2021	06/07/2022	20/08/2022	45.21	1175.65	982.07	0.84	0.30
TR8	05/05/2021	25/04/2022	31/10/2022	188.33	2680.29	814.97	0.31	0.16
TR9	16/06/2021	08/11/2021	02/07/2022	235.63	2805.50	752.44	0.27	0.14
TR10	20/02/2022	25/02/2022	23/03/2022	26.46	812.72	699.85	0.86	0.20

2.2 Lagrangian modeling framework: TrackMPD

The particle trajectories were calculated using a self-modified version of TrackMPD_v2.3, a two dimensional and three-dimensional particle-tracking framework designed for simulating the transport of marine plastic debris in oceans and coastal

105   systems (Jalón-Rojas et al., 2019). This framework supports various formats of current velocity inputs and extends the classic advection-diffusion model by incorporating more complex and realistic particle behaviors and physical processes. For this study, we utilized only the two-dimensional horizontal mode. We selected this framework due to its open-access nature, ease of modification, and flexibility, which make it adaptable to a range of applications. Additionally, it has recently gained significant traction in the field (Baudena et al., 2022; Lin et al., 2024; Rodriguez et al., 2024; Ye et al., 2024).

110   Each particle's position is advected without drag effect using the velocity field provided by the ocean hydrodynamic model. Advection can be computed using the Runge-Kutta method, which supports first-order (Euler Scheme), second-order (RK2), or fourth-order (RK4). The velocity field is interpolated in both time and space at the particle's location, a process that can be computationally time-consuming.

To model turbulent particle movement in horizontal directions, a random-walk model is employed, following Eq. (1) as
115 described by Jalón-Rojas et al. (2019).

$$\vec{x}_{n+1} = \vec{x}_n + R[2K_h \Delta t_i]^{\frac{1}{2}}$$ (1)

where K_h is the horizontal dispersion coefficient (also referred to as horizontal diffusivity) in m²/s, $\vec{x}_n$ is the previous
120 particle position, $\vec{x}_{n+1}$ is the new particle position, R is a random number (with independent values in the two horizontal
directions) having a mean zero and a standard deviation of $r = 1$, and Δt_i is the internal time step.

One of the modifications introduced to the TrackMDP framework was the inclusion of windage effects. This was achieved
by incorporating the wind speed at a height of 10 meters and a windage factor (WDF or wind drift factor) into the differential
equation, as shown in Eq. (2). This approach follows previous modeling applications of the process (Callies et al., 2017;
125 Dagestad and Röhrs, 2019; Kim et al., 2014; Van der Stocken and Menemenlis, 2017). The windage factor accounts for the
influence of surface wind velocity on the object, depending on its shape and size. Typically, WDF values range from 0.01 to
0.06 (1% to 6%) (Abascal et al., 2009; Kim et al., 2014).

Additionally, particles floating on the surface of gravity waves experience a net drift velocity in the direction of wave
propagation, referred to as Stokes drift (Stokes, 1847). This phenomenon was incorporated into the modeling framework as
130 described in Eq. (2), based on prior studies (Sorgente et al., 2016; Tamtare et al., 2022; Zhang et al., 2020).

Thus, Eq. (2), describes the differential equation governing trajectory calculations, excluding the effects of turbulent
diffusion.

$$\frac{d\vec{x}}{dt} = \vec{V}_{current} + \alpha \cdot \vec{V}_{wind} + \vec{V}_{Stokes},$$ (2)

135

where $\vec{V}_{current}$ is the Eulerian ocean current velocity field, $\vec{V}_{wind}$ is the Eulerian wind speed field at a height of 10 meters, α
is the windage factor and $\vec{V}_{Stokes}$ is the Stokes drift velocity.

2.3 Oceanographic and meteorological data

To perform the simulations, multiple oceanographic and meteorological datasets were required depending on the physical
140 processes considered. For the wind field at a height of 10 meters, we used ERA5, the fifth generation ECMWF reanalysis,
which provides global climate and weather data for the past eight decades starting in 1940. ERA5 delivers hourly estimates
for various atmospheric, ocean-wave and land-surface variables, including wind speed and Stokes drift velocity. The dataset
is gridded globally with a horizontal resolution of 0.25º for the atmospheric variables and 0.5º for ocean-wave variables
(Hersbach et al., 2023).

145   For ocean currents velocities, the IBI Ocean Physics Analysis and Forecast dataset from the Copernicus Marine Service was used. The IBI-MFC provides a high-resolution ocean analyses and forecasts with a Level-4 data processing, covering the European waters, specifically the Iberia-Biscay-Ireland (IBI) region, which includes the Canary Islands up to 26ºN. This product is based on an eddy-resolving NEMO model application, offering a horizontal resolution of 0.028º and an hourly temporal resolution.

150   The Stokes drift horizontal velocity field was obtained from the Global Ocean Physics Analysis and Forecast dataset, also provided by the Copernicus Marine Service. This dataset represents the Operational Mercator global ocean analysis and forecast system, with a horizontal resolution of 0.083º. This product offers hourly mean surface fields for Stokes drift velocity, along with other oceanographic variables such as sea level height and daily or monthly temperature.

As these three datasets have different spatial resolutions, their data were linearly interpolated to match with the grid of the

155   IBI Ocean Physics Analysis and Forecast dataset for consistency in the simulations.

2.4 Running simulations

To assess the relative importance of each physical process involved in the trajectory computations and identify the best match with real ocean conditions, we tested combinations of RK2 and RK4 advection schemes, horizontal dispersion coefficients ranging from 0 m^2 /s to 5 m^2 /s, windage factors ranging from 0 to 7%, and the inclusion or exclusion of Stokes

160   drift. This resulted in 32 distinct scenarios (Table 3), yielding a total of 320 simulations (one for each trajectory and scenario), which were then compared to the observed drifters' trajectories.

The 32 scenarios were grouped into four clusters. Scenarios S1 to S8 investigated the importance of the advection scheme and horizontal dispersion coefficient without windage or Stokes drift. Scenarios S9 to S24 studied the effects of the advection scheme, horizontal dispersion and windage. Scenarios S25 to S28 examined the influence of the advection

165   scheme, horizontal dispersion, and Stokes drift. Finally, scenarios S29 to S32 considered all processes, varying the advection scheme and horizontal dispersion.

For the 320 simulations, 100 particles were released at the initial time and position of each of the 10 drifters. The trajectories were computed with an hourly temporal resolution, and their durations were matched to the corresponding drifter data.

170   The simulations were conducted on a computer equipped with 16 GB of RAM and a 12th Gen Intel® Core™ i7-1260P processor, clocked at 2.10 GHz, utilizing four cores for parallel computing.

175

Table 3. Different scenarios (S) considered for the sensitivity analysis of GDP drifters in the Macaronesia region.

Scenario	Advection Scheme	K_h (m² /s)	WDF (%)	Stokes drift
S1	RK4	0	0	No
S2		0.5	0	
S3		2	0	
S4		5	0	
S5	RK2	0	0	
S6		0.5	0	
S7		2	0	
S8		5	0	
S9	RK4	0	1	
S10		1	1	
S11		0	2.5	
S12		1	2.5	
S13		0	5	
S14		1	5	
S15		0	7	
S16		1	7	
S17	RK2	0	1	
S18		1	1	
S19		0	2.5	
S20		1	2.5	
S21		0	5	
S22		1	5	
S23		0	7	
S24		1	7	
S25	RK4	0	0	Yes
S26		1	0	
S27	RK2	0	0	
S28		1	0	
S29	RK4	0	2.5	
S30		1	2.5	
S31	RK2	0	2.5	
S32		1	2.5	

2.5 Evaluation of trajectory modeling

To evaluate and quantify the fit between the modeled and the actual trajectories, a dimensionless dynamical Skill Score is
used, supplemented with visual evaluations. This Skill Score is based on the normalized cumulative Lagrangian separation,
commonly referred to as the Liu-Weisberg Skill Score (Liu and Weisberg, 2011). It has been widely employed to assess the
performance of numerical ocean circulation models, oil-spill tracking models, and similar applications (Coquereau and
Foukal, 2023; Pärt et al., 2023; Röhrs et al., 2012; de Vos et al., 2022). This method measures the separation between real
and modeled trajectories along their entire path, normalized by the total length of the trajectory path, following Eq. (3) by
Liu and Weisberg, (2011).

$$ss = \begin{cases} 1 - \frac{s}{n}, & if \ s \leq n \\ \quad 0, & if \ s > n \end{cases} \tag{3}$$

where n is a tolerance threshold that defines the expectations or requirements for the model. A larger n value corresponds to
lower expectations, while a smaller n value indicates stricter requirements. The variable s is and index defined as the average
separation distance weighted by the cumulative length of the observed trajectory, as describe in Eq. (4).

$$s = \frac{\sum_{i=1}^{N} d_i}{\sum_{i=1}^{N} l_i}, \tag{4}$$

where N is the total number of time steps, d is the separation distance, l is the length of the observed trajectory and i is the
index indicating the time step at which d and l were calculated.

We used a tolerance threshold $n=1$, following previous applications of this Skill Score (Jalón-Rojas et al., 2019; Liu et al.,
2014; Révelard et al., 2021; Röhrs et al., 2012).

A Skill Score of zero indicates no similarities between trajectories, while a value of one indicates that the trajectories are
equivalent. To visualize the distribution of the Skill Scores across scenarios and parameter values, we employed boxplots.
These boxplots illustrate the median (center line of the box), the 1st quartile (lower border of the box), and the 3rd quartile
(upper border of the box), as well as potential outliers. The lower and upper whiskers extend to the range of the data within
1.5 times the interquartile range (IQR) from the 1st and 3rd quartiles, respectively.

3 Results and discussion

3.1 Differences across scenarios

Figure 2 presents the Skill Score results obtained from the simulations corresponding to each scenario in Table 3. Significant
differences between scenarios are evident. In particular, in the first eight scenarios, where the windage factor (WDF) and

Stokes drift were excluded, the medians of the Skill Scores remain low, close to zero. However, beginning with S9, the Skill Scores increase substantially, with medians exceeding 0.5. This improvement aligns with simulations that incorporate wind forcing and/or Stokes drift.
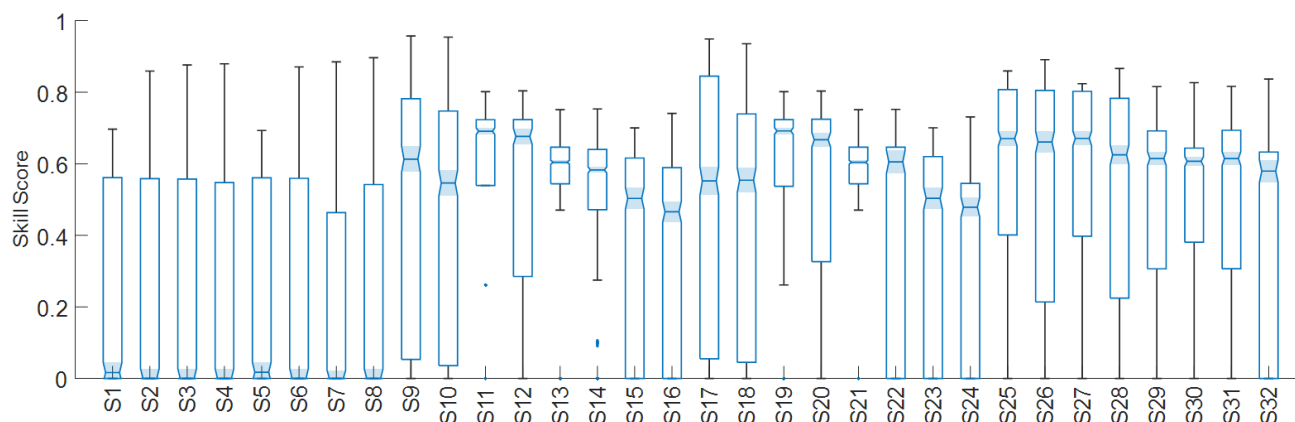
210 **Figure 2. Boxplot representation of the Skill Scores (n=1) obtained for the trajectories evaluated in each scenario defined in Table 3. Shaded areas represent the 95% confidence intervals around the median. The horizontal line within each box indicates the median, while the box boundaries correspond to the interquartile range (IQR). The whiskers extend to the smallest values within 1.5 times the IQR, and individual points outside this range represent potential outliers.**

3.2 Turbulent diffusion

215 In terms of horizontal dispersion, no noticeable differences are observed between scenarios S1-S8 (Figure 2), where horizontal dispersion was specifically analyzed. Similarly, in the remaining simulations, where horizontal dispersion coefficient has been alternated between 0 and 1 m^2/s, no significant differences were identified. The apparent insensitivity of the simulated trajectories to turbulent diffusion may be attributed to the drifters not being substantially influenced by highly nonlinear processes. This aligns with the premise that including horizontal dispersion in particle simulations is
220 intended to stochastically approximate the effects of such nonlinear dynamics.

However, most trajectories originating from the northern area of the region - TR2, TR5, TR7, TR8, TR9 and TR10 (Figure 1), which are primarily influenced by the Canary Current, show greater variability in their Skill Scores (Figure 3). These trajectories often exhibit meanders and are likely to encounter low-speed conditions, where horizontal dispersion plays a more significant role in trajectory calculations, leading to increased variability in Skill Scores.

225 ### 3.3 Advection scheme

Concerning the advection schemes employed, no significant differences in the median Skill Score are generally observed between the two numerical methods, except for certain trajectories, such as TR1, where RK4 appears to yield higher Skill Scores (Figure 3). A particularly notable case is TR6, where the drifter is influenced by a mesoscale eddy south of Madeira (Figure 1). In this instance, RK4 exhibits lower variability and a considerably higher third quartile (Figure 3). However, it is

230 important to note that a visual comparison between the observed TR6 trajectory (Figure 1) and the simulated trajectory (not shown) reveals that the circular movements induced by the eddy are not fully replicated. After three rotations, the virtual particles exit the eddy structure, whereas the drifter remains within the eddy for at least ten rotations.
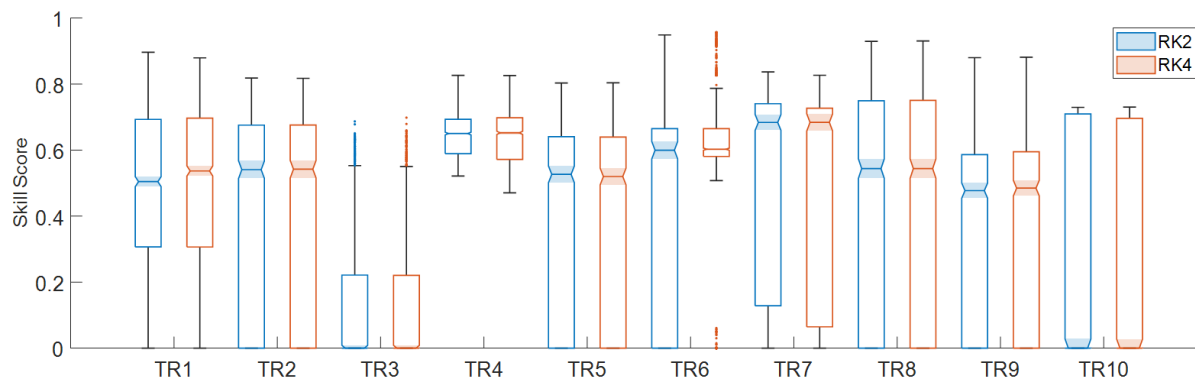
Figure 3. Boxplot representation of the Skill Scores (n=1) obtained for the studied trajectories comparing results using 2nd Order Runge-Kutta (RK2) and 4th Order Runge-Kutta (RK4) methods. Shaded areas represent the 95% confidence interval around the median.

The results suggest that, in general, there are not significant differences between the advection schemes. However, specific cases, such as TR6, indicate that RK4 yields better results. This appears to be particularly true in regions where mesoscale

240 activity predominates. These findings imply that in the Macaronesia region, where mesoscale processes play a significant role, RK4 is the more suitable advection scheme.

3.4 Windage effect

This sensitivity analysis highlights the importance of windage in trajectory calculations, as notable improvements are observed when wind forcing is included (Figure 2). However, substantial variations in performance are evident depending on

245 the WDF. Generally, Skill Scores improve when wind forcing is incorporated with a specific WDF, reaching a peak at values between 2.5 and 5% (with the exception of TR3). This finding aligns with previous studies utilizing drifters (De Dominicis et al., 2016; Pärt et al., 2023; Poulain et al., 2009).

Examining the Skill Score performance for individual trajectories (Figure 4), reveals notable differences. For TR1, a slight improvement is observed at a WDF of 1%, but higher values lead to reduced performance. The Skill Scores for TR2 and

250 TR10 show a significant improvement as the WDF increases up to 2.5%, followed by a decline at higher values, although TR10 does not exhibit differences between 2.5% and 5%. TR3 remains an outlier, where the inclusion of any wind forcing results in Skill Scores of zero. For TR4, the Skill Scores improve significantly with wind forcing and remain relatively constant across varying WDFs, with a slight peak at 7%. The performance of simulated TR5 and TR7 improves progressively, peaking at WDF values of 2.5% and 5%, respectively. The simulated TR6 shows no significant differences

255 between WDF values, except for a slightly better fit at 1%. Finally, the Skill Scores for TR8 and TR9 display similar patterns, with marked improvement when wind forcing is included at WDF=1%, followed by a decline at higher values, stabilizing at approximately 0.5. These differing behaviors may result from various factors, such as morphological characteristics of the buoys, particularly their shape and diameter. Additionally, the optimal WDF may depend on wind intensity, as noted in other studies (De Dominicis et al., 2016).
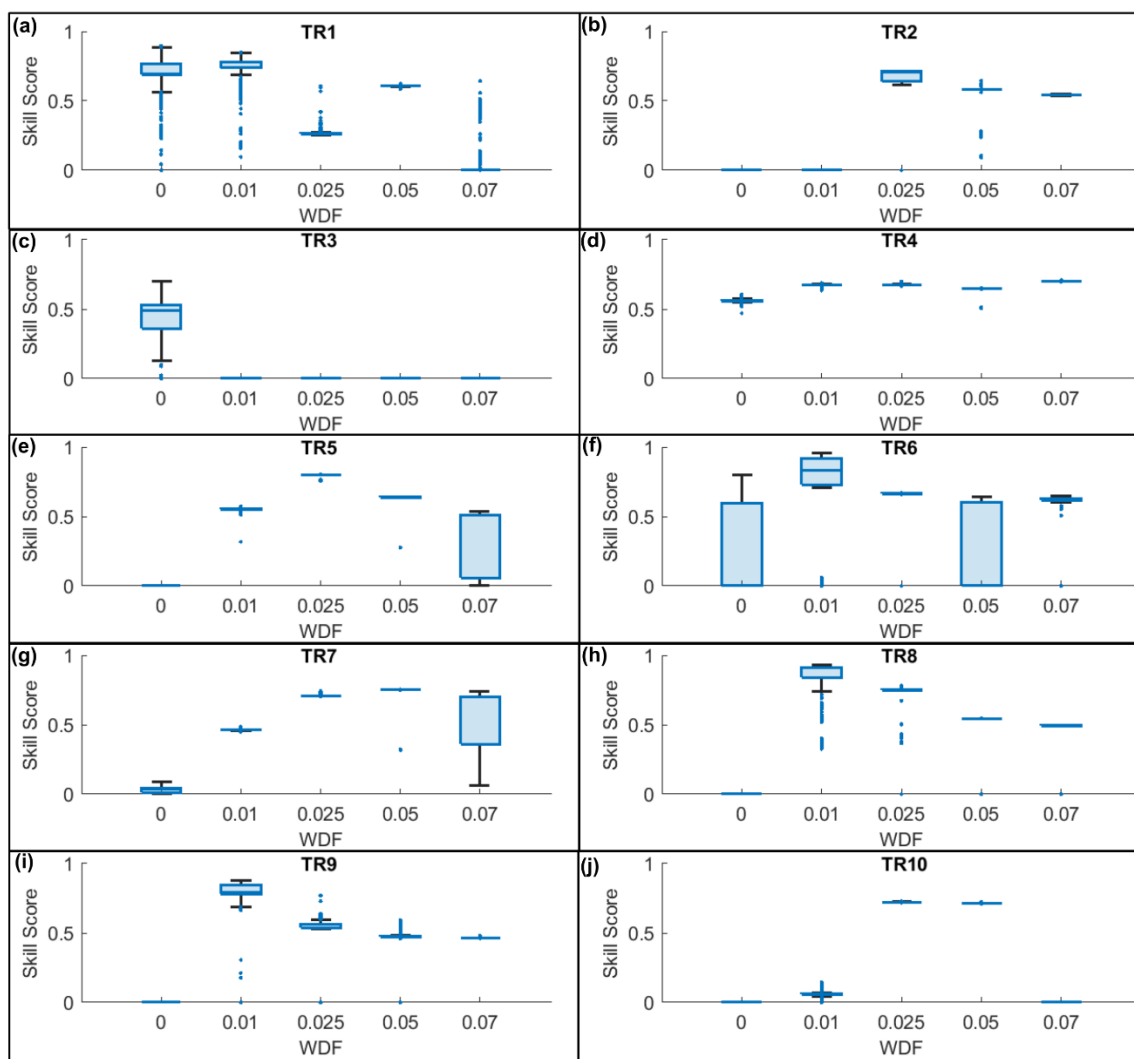
Figure 4. Boxplot representation of the Skill Scores (n=1) obtained for each trajectory under varying windage factors.

3.5 Stokes drift

Regarding the Stokes drift, it is noteworthy in Fig. 5 that simulations incorporating this process (S25-S32) yield higher median Skill Scores compared to those where it is omitted. When the Stokes drift is included without accounting for windage

265 (Figure 5a), improvements are observed for TR2, TR4, TR7, TR8, TR9 and TR10. When the Stokes drift and windage are combined with a WDF of 2.5% (Figure 5b), similar improvements are observed for certain cases (TR1, TR6 and TR7), but there is a greater variability overall compared to simulations excluding Stokes drift. This likely occurs because the drift induced by waves often aligns with wind direction, producing an effect similar to windage. Consequently, it can be argued that the WDF implicitly incorporates the Stokes drift caused by wind waves (van den Bremer and Breivik, 2018; Callies et

270 al., 2017; Korotenko et al., 2010). This also explains why optimal WDF values depend on whether the Stokes drift is included (Dagestad and Röhrs, 2019).

Furthermore, this relationship clarifies why, when windage is considered, there are no substantial differences between the inclusion and omission of the Stokes drift (Figure 5). However, generalizing wind and wave forcing may not be appropriate in regions where swell is significant, as it can have a different direction from the prevailing wind. Additionally, the

275 implementation of Stokes drift in trajectory computation frameworks requires further research. Among other factors, the significance of this process has been shown to vary depending on the region and time of year (Rühs et al., 2024).
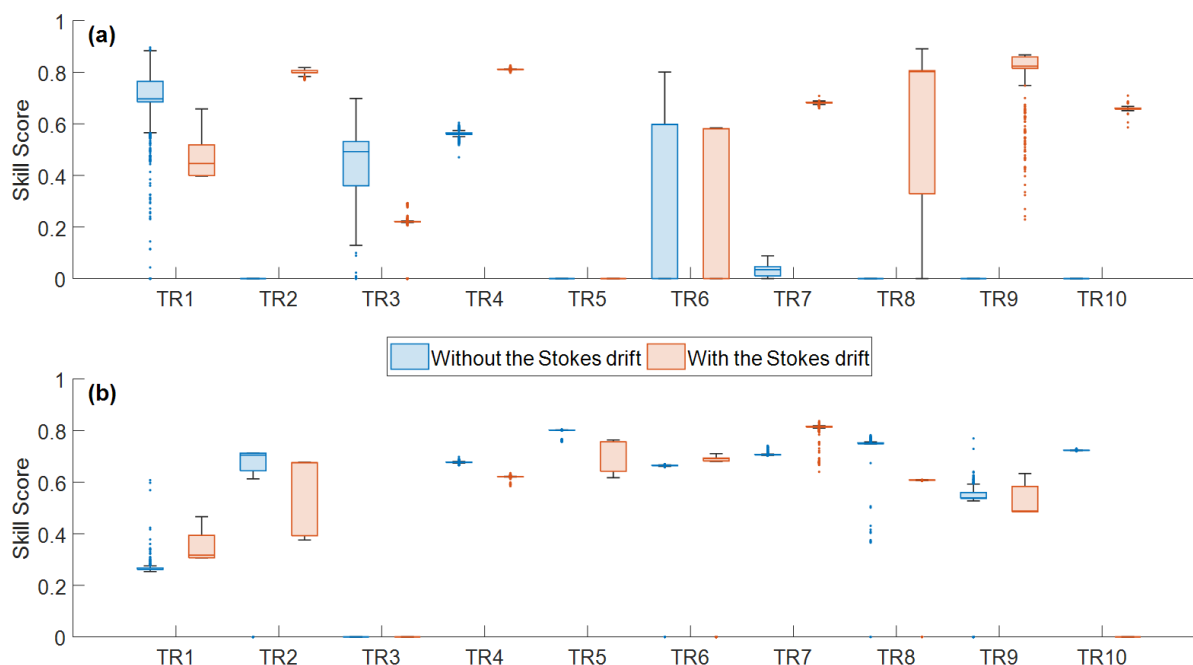
Figure 5. Boxplot representation of the Skill Scores (n=1) obtained for each trajectory comparing the inclusion and omission of the
280 **Stokes drift (a) without considering windage and (b) with a windage factor of 2.5%.**

3.6 Singular cases

On the one hand, trajectory TR3 stands out as particularly challenging to replicate due to its anomalous displacement (Figure 1). This trajectory ocurred from late December 2021 to early February 2022, a period characterized by significant dust cloud activity. Notably, January 2022 ranked among the top three Januarys with the highest *calima* occurrence since 1974

285   (Agencia Estatal de Meteorología, 2022). It is possible that this phenomenon was not adequately represented in the wind model. Additionally, the drifter's trajectory may have been influenced by an upwelling filament (not shown), which could explain the worsened results when wind forcing was included in the simulations. A third potential explanation is that the start date of the trajectory coincides with the date of drogue loss (Table 2). A failure in the strain gauge may have resulted in the drogue remaining intact, at least during the initial days of the trajectory, preventing the drifter from being significantly
290   affected by the wind.

On the other hand, the low Skill Scores obtained for TR10 (Figure 3) could be attributed to its location on the African continental shelf (Figure 1). In this region, physical processes such as the upwelling and the Canary Upwelling Current, may introduce complexities that challenge the accuracy of the IBI Ocean Physics Analysis and Forecast model.

4. Conclusions

295   We conducted a sensitivity analysis to evaluate the influence of various physical processes on the transport of undrogued surface drifters mimicking marine litter in the upper ocean. This analysis considered different advection schemes, horizontal dispersion coefficients, and the impacts of windage and Stokes drift processes. Our findings highlight that windage and Stokes drift significantly improve the accuracy of trajectory simulations, particularly when included in the model from scenario S9 onward.

300   The analysis of horizontal dispersion showed that trajectory simulations were generally not significantly affected by variations in the dispersion coefficients.

Regarding advection schemes, both RK2 and RK4 produced comparable results; however, RK4 demonstrated greater accuracy in cases involving pronounced mesoscale activity. This suggests that, in regions like Macaronesia with a notable mesoscale activity, RK4 may provide a more precise representation of drifter trajectories.

305   In the upper ocean, windage emerged as a dominant factor in the Canary Current System, while Stokes drift exhibited an implicit effect.

The most reliable results were obtained when windage was applied within a range of 2.5-5% with differences linked to varying weather conditions.

Finally, TrackMPD has proven to be an effective tool for simulating and analyzing the trajectory of undrogued surface
310   drifters mimicking marine litter traveling under various conditions, providing valuable insights for identifying marine debris hotspots and managing marine pollution crises. However, selecting the appropriate parameters in TrackMPD to generate accurate virtual trajectories under different environmental conditions requires a thorough understanding of the study area and the characteristics of the target object.

315   *Data availability.* The datasets used in this study are publicly available. Oceanographic data were obtained from Copernicus Marine Service. Specifically, the Eulerian ocean currents were provided by the IBI Ocean Physics Analysis and Forecast

product (https://doi.org/10.48670/moi-00027, E.U. Copernicus Marine Service Product, 2024b). Additionally, Stokes drift data were provided by the Global Ocean Physics Analysis and Forecast dataset (https://doi.org/10.48670/moi-00016, E.U. Copernicus Marine Service Product, 2024a). Meteorological data regarding wind speed were sourced from the ERA5 product (https://doi.org/10.24381/cds.adbb2d47, Hersbach et al., 2023). Drifter data were obtained from the Global Drifter Program (https://doi.org/10.25921/x46c-3620, Elipot et al., 2022)

Code availability. The TrackMPD framework is available in GitHub (https://github.com/IJalonRojas/TrackMPD) thanks to Jalón-Rojas et al. (2019). The modifications implemented by the authors include adapting the 2D horizontal mode of TrackMPD to utilize current data from IBI Ocean Physics Analysis and Forecasts. Additionally, windage and Stokes drift have been incorporated as described in the manuscript. For greater computational efficiency, instead of interpolating bathymetry data at every particle position, the nearest neighbour method is used. The modified code is available upon request to the corresponding authors.

Authors contributions. AC: Conceptualization, Data Curation, Methodology, Visualization, Formal Analysis, Writing-original draft, Writing-review & editing. FM: Conceptualization, Dara Curation, Methodology, Visualization, Supervision, Writing-review & editing. DVM: Conceptualization, Visualization, Funding acquisition, Supervision, Writing-review & editing. EFN: Conceptualization Methodology, Visualization, Funding acquisition, Supervision, Writing-review & editing. BAG: Conceptualization, Data Curation, Methodology, Visualization, Supervision, Writing-review & editing.

Competing interests. The authors declare that they have no conflict of interest.

References

Abascal, A. J., Castanedo, S., Mendez, F. J., Medina, R., and Losada, I. J.: Calibration of a Lagrangian Transport Model Using Drifting Buoys Deployed during the "Prestige" Oil Spill, Journal of Coastal Research, Vol 25, No. 1, 25, 80–90, 2009.

Agencia Estatal de Meteorología: AVANCE CLIMATOLÓGICO DE CANARIAS ENERO 2022, Las Palmas de Gran Canaria/Santa Cruz de Tenerife, 2022.

Arístegui, J., Tett, P., Hernández-Guerra, A., Basterretxea, G., Montero, M. F., Wild, K., Sangrà, P., Hernández-León, S.,
350   Cantón, M., García-Braun, J. A., Pacheco, M., and Barton, E. D.: The influence of island-generated eddies on chlorophyll
distribution: a study of mesoscale variation around Gran Canaria, Deep Sea Research Part I: Oceanographic Research
Papers, 44, 71–96, https://doi.org/10.1016/S0967-0637(96)00093-3, 1997.

Bakun, A. and Nelson, C. S.: The Seasonal Cycle of Wind-Stress Curl in Subtropical Eastern Boundary Current Regions, J
Phys Oceanogr, 21, 1815–1834, https://doi.org/10.1175/1520-0485(1991)021<1815:TSCOWS>2.0.CO;2, 1991.

355   Barton, E. D., Arístegui, J., Tett, P., Canton, M., García-Braun, J., Hernández-León, S., Nykjaer, L., Almeida, C., Almunia,
J., Ballesteros, S., Basterretxea, G., Escanez, J., García-Weill, L., Hernández-Guerra, A., López-Laatzen, F., Molina, R.,
Montero, M. F., Navarro-Peréz, E., Rodríguez, J. M., Van Lenning, K., Vélez, H., and Wild, K.: The transition zone of
the Canary Current upwelling region, Prog Oceanogr, 41, 455–504, https://doi.org/10.1016/S0079-6611(98)00023-8,
1998.

360   Barton, E. D., Basterretxea, G., Flament, P., Mitchelson-Jacob, E. G., Jones, B., Arístegui, J., and Herrera, F.: Lee region of
Gran Canaria, J Geophys Res Oceans, 105, 17173–17193, https://doi.org/10.1029/2000JC900010, 2000.

Basterretxea, G., Barton, E. D., Tett, P., Sangrà, P., Navarro-Perez, E., and Arístegui, J.: Eddy and deep chlorophyl
maximum response to wind-shear in the lee of Gran Canaria, Deep Sea Research Part I: Oceanographic Research Papers,
49, 1087–1101, https://doi.org/10.1016/S0967-0637(02)00009-2, 2002.

365   Baudena, A., Ser-Giacomi, E., Jalón-Rojas, I., Galgani, F., and Pedrotti, M. L.: The streaming of plastic in the Mediterranean
Sea, Nature Communications 2022 13:1, 13, 1–9, https://doi.org/10.1038/s41467-022-30572-5, 2022.

van den Bremer, T. S. and Breivik: Stokes drift, Philosophical Transactions of the Royal Society A: Mathematical, Physical
and Engineering Sciences, 376, https://doi.org/10.1098/RSTA.2017.0104, 2018.

Brügge, B. and Dengg, J.: Differences in drift behavior between drogued and undrogued satellite-tracked drifting buoys, J
370   Geophys Res Oceans, 96, 7249–7263, https://doi.org/10.1029/90JC02667, 1991.

Callies, U., Groll, N., Horstmann, J., Kapitza, H., Klein, H., Maßmann, S., and Schwichtenberg, F.: Surface drifters in the
German Bight: model validation considering windage and Stokes drift, Ocean Science, 13, 799–827,
https://doi.org/10.5194/os-13-799-2017, 2017.

Castro-Rosero, L. M., Hernandez, I., Alsina, J. M., and Espino, M.: Transport and accumulation of floating marine litter in
375   the Black Sea: insights from numerical modeling, Front Mar Sci, 10, 1213333,
https://doi.org/10.3389/FMARS.2023.1213333/BIBTEX, 2023.

Coquereau, A. and Foukal, N. P.: Evaluating altimetry-derived surface currents on the south Greenland shelf with surface
drifters, Ocean Science, 19, 1393–1411, https://doi.org/10.5194/OS-19-1393-2023, 2023.

Cropper, T. E., Hanna, E., and Bigg, G. R.: Spatial and temporal seasonal trends in coastal upwelling off Northwest Africa,
380   1981–2012, Deep Sea Research Part I: Oceanographic Research Papers, 86, 94–111,
https://doi.org/10.1016/J.DSR.2014.01.007, 2014.

Dagestad, K.-F. and Röhrs, J.: Prediction of ocean surface trajectories using satellite derived vs. modeled ocean currents, Remote Sens Environ, 223, 130–142, https://doi.org/10.1016/j.rse.2019.01.001, 2019.

Dagestad, K.-F., Röhrs, J., Breivik, Ø., and Ådlandsvik, B.: OpenDrift v1.0: a generic framework for trajectory modelling, Geosci Model Dev, 11, 1405–1420, https://doi.org/10.5194/gmd-11-1405-2018, 2018.

Declerck, A., Delpey, M., Rubio, A., Ferrer, L., Basurko, O. C., Mader, J., and Louzao, M.: Transport of floating marine litter in the coastal area of the south-eastern Bay of Biscay: A Lagrangian approach using modelling and observations, Journal of Operational Oceanography, 12, S111–S125, https://doi.org/10.1080/1755876X.2019.1611708, 2019.

De Dominicis, M., Bruciaferri, D., Gerin, R., Pinardi, N., Poulain, P. M., Garreau, P., Zodiatis, G., Perivoliotis, L., Fazioli, L., Sorgente, R., and Manganiello, C.: A multi-model assessment of the impact of currents, waves and wind in modelling surface drifters and oil spill, Deep Sea Research Part II: Topical Studies in Oceanography, 133, 21–38, https://doi.org/10.1016/j.dsr2.2016.04.002, 2016.

Elipot, S., Lumpkin, R., Perez, R. C., Lilly, J. M., Early, J. J., and Sykulski, A. M.: A global surface drifter data set at hourly resolution, J Geophys Res Oceans, 121, 2937–2966, https://doi.org/10.1002/2016JC011716, 2016.

Elipot, S., Sykulski, A., Lumpkin, R., Centurioni, L., and Pazos, M.: Hourly location, current velocity, and temperature collected from Global Drifter Program drifters world-wide, https://doi.org/10.25921/x46c-3620, 2022.

E.U. Copernicus Marine Service Product: Global Ocean Physics Analysis and Forecast, https://doi.org/10.48670/moi-00016, 2024a.

E.U. Copernicus Marine Service Product: Atlantic-Iberian Biscay Irish- Ocean Physics Analysis and Forecast, https://doi.org/10.48670/moi-00027, 2024b.

Fredj, E., Carlson, D. F., Amitai, Y., Gozolchiani, A., and Gildor, H.: The particle tracking and analysis toolbox (PaTATO) for Matlab, Limnol Oceanogr Methods, 14, 586–599, https://doi.org/10.1002/LOM3.10114, 2016.

Hernández Guerra, A.: Estructuras oceanográficas observadas en las aguas que rodean las Islas Canarias mediante escenas de los sensores AVHRR y CZCS, Universidad de Las Palmas de Gran Canaria, 1990.

Hernández-Guerra, A., Machín, F., Antoranz, A., Cisneros-Aguirre, J., Gordo, C., Marrero-Díaz, A., Martínez, A., Ratsimandresy, A. W., Rodríguez-Santana, A., Sangrá, P., López-Laazen, F., Parrilla, G., and Pelegrí, J. L.: Temporal variability of mass transport in the Canary Current, Deep Sea Research Part II: Topical Studies in Oceanography, 49, 3415–3426, https://doi.org/10.1016/S0967-0645(02)00092-9, 2002.

Hersbach, H., Bell, B., Berrisford, P., Biavati, G., Horányi, A., Muñoz Sabater, J., Nicolas, J., Peubey, C., Radu, R., Rozum, I., Schepers, D., Simmons, A., Soci, C., Dee, D., and Thépaut, J.-N.: ERA5 hourly data on single levels from 1940 to present. Copernicus Climate Change Service (C3S) Climate Data Store (CDS), https://doi.org/10.24381/cds.adbb2d47, 2023.

Jalón-Rojas, I., Wang, X. H., and Fredj, E.: A 3D numerical model to Track Marine Plastic Debris (TrackMPD): Sensitivity of microplastic trajectories and fates to particle dynamical properties and physical processes, Mar Pollut Bull, 141, 256–272, https://doi.org/10.1016/j.marpolbul.2019.02.052, 2019.

Kim, T.-H., Yang, C.-S., Oh, J.-H., and Ouchi, K.: Analysis of the Contribution of Wind Drift Factor to Oil Slick Movement under Strong Tidal Condition: Hebei Spirit Oil Spill Case, PLoS One, 9, e87393, https://doi.org/10.1371/journal.pone.0087393, 2014.

Korotenko, K. A., Bowman, M. J., and Dietrich, D. E.: High-resolution numerical model for predicting the transport and dispersal of oil spilled in the black sea, Terrestrial, Atmospheric and Oceanic Sciences, 21, 123–136, https://doi.org/10.3319/TAO.2009.04.24.01(IWNOP), 2010.

Lange, M. and Sebille, E. Van: Parcels v0.9: Prototyping a Lagrangian ocean analysis framework for the petascale age, Geosci Model Dev, 10, 4175–4186, https://doi.org/10.5194/GMD-10-4175-2017, 2017.

Lin, H., Yu, W., and Lian, Z.: Influence of Ocean Current Features on the Performance of Machine Learning and Dynamic Tracking Methods in Predicting Marine Drifter Trajectories, Journal of Marine Science and Engineering 2024, Vol. 12, Page 1933, 12, 1933, https://doi.org/10.3390/JMSE12111933, 2024.

Liu, Y. and Weisberg, R. H.: Evaluation of trajectory modeling in different dynamic regions using normalized cumulative Lagrangian separation, J Geophys Res Oceans, 116, 9013, https://doi.org/10.1029/2010JC006837, 2011.

Liu, Y., Weisberg, R. H., Vignudelli, S., and Mitchum, G. T.: Evaluation of altimetry-derived surface current products using Lagrangian drifter trajectories in the eastern Gulf of Mexico, J Geophys Res Oceans, 119, 2827–2842, https://doi.org/10.1002/2013JC009710, 2014.

Machín, F. and Pelegrí, J. L.: Effect of the Canary Islands in the blockage and mixing of the North Atlantic eastern water masses, Geophys Res Lett, 33, 4605, https://doi.org/10.1029/2005GL025048, 2006.

Machín, F. and Pelegrí, J. L.: Northward Penetration of Antarctic Intermediate Water off Northwest Africa, J Phys Oceanogr, 39, 512–535, https://doi.org/10.1175/2008JPO3825.1, 2009.

Machín, F., Hernández-Guerra, A., and Pelegrí, J. L.: Mass fluxes in the Canary Basin, Prog Oceanogr, 70, 416–447, https://doi.org/10.1016/J.POCEAN.2006.03.019, 2006.

Mason, E., Colas, F., Molemaker, J., Shchepetkin, A. F., Troupin, C., McWilliams, J. C., and Sangrà, P.: Seasonal variability of the Canary Current: A numerical study, J Geophys Res Oceans, 116, https://doi.org/10.1029/2010JC006665, 2011.

McGlade, J., Samy Fahim, I., Green, D., Landrigan, P., Andrady, A., Costa, M., Geyer, R., Gomes, R., Tan Shau Hwai, A., Jambeck, J., Li, D., Rochman, C., Ryan, P., Thiel, M., Thompson, R., Townsend, K., and Turra, A.: From Pollution To Solution: a global assessment of marine litter and plastic pollution, 2021.

Navarro-Pérez, E. and Barton, E. D.: Seasonal and interannual variability of the Canary Current, Sci Mar, 65, 205–213, https://doi.org/10.3989/SCIMAR.2001.65S1205, 2001.

Pärt, S., Björkqvist, J.-V., Alari, V., Maljutenko, I., and Uiboupin, R.: An ocean-wave-trajectory forecasting system for the eastern Baltic Sea: Validation against drifting buoys and implementation for oil spill modeling, Mar Pollut Bull, 195, https://doi.org/10.1016/j.marpolbul.2023.115497, 2023.

Pazan, S. E.: Intercomparison of drogued and undrogued drift buoys, Oceans Conference Record (IEEE), 2, 864–872, https://doi.org/10.1109/OCEANS.1996.568343, 1996.

450 Pelegrí, J. L., Arístegui, J., Cana, L., González-Dávila, M., Hernández-Guerra, A., Hernández-León, S., Marrero-Díaz, A., Montero, M. F., Sangrà, P., and Santana-Casiano, M.: Coupling between the open ocean and the coastal upwelling region off northwest Africa: water recirculation and offshore pumping of organic matter, Journal of Marine Systems, 54, 3–37, https://doi.org/10.1016/J.JMARSYS.2004.07.003, 2005.

Pelegrí, J. L., Marrero-Díaz, A., and Ratsimandresy, A. W.: Nutrient irrigation of the North Atlantic, Prog Oceanogr, 70,
455 366–406, https://doi.org/10.1016/J.POCEAN.2006.03.018, 2006.

Pérez-Hernández, M. D., Hernández-Guerra, A., Fraile-Nuez, E., Comas-Rodríguez, I., Benítez-Barrios, V. M., Domínguez-Yanes, J. F., Vélez-Belchí, P., and De Armas, D.: The source of the Canary current in fall 2009, J Geophys Res Oceans, 118, 2874–2891, https://doi.org/10.1002/JGRC.20227, 2013.

Poulain, P. M., Gerin, R., Mauri, E., and Pennel, R.: Wind effects on drogued and undrogued drifters in the eastern
460 Mediterranean, J Atmos Ocean Technol, 26, 1144–1156, https://doi.org/10.1175/2008JTECHO618.1, 2009.

Révelard, A., Reyes, E., Mourre, B., Hernández-Carrasco, I., Rubio, A., Lorente, P., Fernández, C. D. L., Mader, J., Álvarez-Fanjul, E., and Tintoré, J.: Sensitivity of Skill Score Metric to Validate Lagrangian Simulations in Coastal Areas: Recommendations for Search and Rescue Applications, Front Mar Sci, 8, 630388, https://doi.org/10.3389/FMARS.2021.630388/BIBTEX, 2021.

465 Rodriguez, C., Silva, P., Moreira, L., Zacher, L., Fernandes, A., Bouyssou, R., Jalón-Rojas, I., Moller, O., Garcia-Rodriguez, F., Pinho, G. L. L., and Fernandes, E.: Trajectory, fate, and magnitude of continental microplastic loads to the inner shelf: A case study of the world's largest coastal shallow lagoon, Science of The Total Environment, 948, 174791, https://doi.org/10.1016/J.SCITOTENV.2024.174791, 2024.

Röhrs, J., Christensen, K. H., Hole, L. R., Broström, G., Drivdal, M., and Sundby, S.: Observation-based evaluation of
470 surface wave effects on currents and trajectory forecasts, Ocean Dyn, 62, 1519–1533, https://doi.org/10.1007/S10236-012-0576-Y/FIGURES/7, 2012.

Rühs, S., Sebille, E. van, Moulin, A., Clementi, E., and Bremer, T. van den: Non-negligible impact of Stokes drift and wave-driven Eulerian currents on simulated surface particle dispersal in the Mediterranean Sea, EGU24, https://doi.org/10.5194/EGUSPHERE-EGU24-13046, 2024.

475 Sangrà, P., Pascual, A., Rodríguez-Santana, A., Machín, F., Mason, E., Mcwilliams, J. C., Pelegrí, J. L., Dong, C., Rubio, A., Arístegui, J., Marrero-Díaz, A., Hern Andez-Guerra, A., Martínez-Marrero, A., and Auladell, M.: The Canary Eddy Corridor: A major pathway for long-lived eddies in the subtropical North Atlantic, Deep Sea Research Part I: Oceanographic Research Papers, https://doi.org/10.1016/j.dsr.2009.08.008, 2009.

Sorgente, R., Tedesco, C., Pessini, F., De Dominicis, M., Gerin, R., Olita, A., Fazioli, L., Di Maio, A., and Ribotti, A.:
480 Forecast of drifter trajectories using a Rapid Environmental Assessment based on CTD observations, Deep Sea Research Part II: Topical Studies in Oceanography, 133, 39–53, https://doi.org/10.1016/J.DSR2.2016.06.020, 2016.

Van der Stocken, T. and Menemenlis, D.: Modelling mangrove propagule dispersal trajectories using high-resolution estimates of ocean surface winds and currents, Biotropica, 49, 472–481, https://doi.org/10.1111/BTP.12440, 2017.

Stokes, G. G.: On the Theory of Oscillatory Waves, Transactions of the Cambridge Philosophical Society, 8, 441–455, 1847.

485 Stramma, L. and Siedler, G.: Seasonal changes in the North Atlantic subtropical gyre, J Geophys Res Oceans, 93, 8111–8118, https://doi.org/10.1029/JC093IC07P08111, 1988.

Tamtare, T., Dumont, D., and Chavanne, C.: The Stokes drift in ocean surface drift prediction, Journal of Operational Oceanography, 15, 156–168, https://doi.org/10.1080/1755876X.2021.1872229, 2022.

Torres-Padrón, M. E., Gelado-Caballero, M. D., Collado-Sánchez, C., Siruela-Matos, V. F., Cardona-Castellano, P. J., and

490 Hernández-Brito, J. J.: Variability of dust inputs to the CANIGO zone, Deep Sea Research Part II: Topical Studies in Oceanography, 49, 3455–3464, https://doi.org/10.1016/S0967-0645(02)00091-7, 2002.

de Vos, M., Barnes, M., Biddle, L. C., Swart, S., Ramjukadh, C. L., and Vichi, M.: Evaluating numerical and free-drift forecasts of sea ice drift during a Southern Ocean research expedition: An operational perspective, Journal of Operational Oceanography, 15, 187–203, https://doi.org/10.1080/1755876X.2021.1883293, 2022.

495 Ye, P., Huang, D., Xuan, J., and He, S.: Patterns and mechanism of wintertime penetrating fronts in the East China Sea, Sci China Earth Sci, 67, 3500–3514, https://doi.org/10.1007/S11430-023-1433-X/METRICS, 2024.

Zhang, X., Cheng, L., Zhang, F., Wu, J., Li, S., Liu, J., Chu, S., Xia, N., Min, K., Zuo, X., and Li, M.: Evaluation of multi-source forcing datasets for drift trajectory prediction using Lagrangian models in the South China Sea, Applied Ocean Research, 104, 102395, https://doi.org/10.1016/J.APOR.2020.102395, 2020.

500